Quarterly Technical Report

Growth, Characterization and Device Development in Monocrystalline Diamond Films

Supported under Grant #N00014-93-I-0437
Office of the Chief of Naval Research
Report for the period 10/1/96–12/31/96

R. F. Davis, R. J. Nemanich* and Z. Sitar
P. K. Baumann*, S. P. Bozeman, S. K. Han,
M. T. McClure, B. L. Ward*, and C. A. Wolden
North Carolina State University
c/o Materials Science and Engineering Department
*Department of Physics
Box 7907
Raleigh, NC 27695

December, 1996

REPORT DOCUMENTATION PAGE

Form Approved
OMB No. 0704-0188

1. AGENCY USE ONLY *(Leave blank)*	2. REPORT DATE	3. REPORT TYPE AND DATES COVERED
	December, 1996	Quarterly Technical 10/1/96-12/31/96

4. TITLE AND SUBTITLE

Growth, Characterization and Device Development in Monocrystalline Diamond Films

5. FUNDING NUMBERS

s400003srr14
1114SS
N00179
N66005
4B855

6. AUTHOR(S)

R. F. Davis, R. J. Nemanich, and Z. Sitar

7. PERFORMING ORGANIZATION NAME(S) AND ADDRESS(ES)

North Carolina State University
Hillsborough Street
Raleigh, NC 27695

8. PERFORMING ORGANIZATION REPORT NUMBER

N00014-93-I-0437

9. SPONSORING/MONITORING AGENCY NAMES(S) AND ADDRESS(ES)

Sponsoring: ONR, Code 312, 800 N. Quincy, Arlington, VA 22217-5660
Monitoring: Admin. Contracting Officer, ONR, Regional Office Atlanta
101 Marietta Tower, Suite 2805
101 Marietta Street
Atlanta, GA 30323-0008

10. SPONSORING/MONITORING AGENCY REPORT NUMBER

11. SUPPLEMENTARY NOTES

12a. DISTRIBUTION/AVAILABILITY STATEMENT

Approved for Public Release; Distribution Unlimited

12b. DISTRIBUTION CODE

13. ABSTRACT ***(Maximum 200 words)***

The electron affinity and Schottky barrier height of thin Cu and Zr films on diamond (100) substrates, cleaned at 500° or 1150°C in UHV and terminated with oxygen or free of chemisorbed species, respectively, were correlated by means of UV photoemission spectroscopy. The achievement of NEA was dependent on the surface preparation before metal deposition and on the metal work function. The Schottky barrier height for clean surfaces was lower than those terminated by oxygen; the former exhibited an NEA. In all field emission measurements, a reduction in the threshold electric field was observed upon metal overgrowth. Free-standing, 4 mm diameter highly-textured (100) diamond membranes were obtained by coupling bias enhanced nucleation in a microwave plasma CVD reactor with an evolutionary texture selection growth process in a low pressure combustion flame reactor and subsequent etching of the Si substrate. High energy particle detectors were fabricated via patterning of microstrip electrodes on these membranes. These detectors were used to measure the energy spectra of α-particles at the Continuous Electron Beam Accelerator Facility and to determine the spatial resolution of these particles. The performance was similar to those obtained by monocrystalline detectors.

14. SUBJECT TERMS

negative electron affinity, Schottky barrier height, metal-diamond interfaces, UV photoemission spectroscopy, diamond, membranes, bias enhanced nucleation, microwave plasma, CVD, combustion flame, particle detector, microstrip electrode, α-particle, energy spectra, spatial resolution

15. NUMBER OF PAGES

17

16. PRICE CODE

17. SECURITY CLASSIFICATION OF REPORT	18. SECURITY CLASSIFICATION OF THIS PAGE	19. SECURITY CLASSIFICATION OF ABSTRACT	20. LIMITATION OF ABSTRACT
UNCLAS	UNCLAS	UNCLAS	SAR

Table of Contents

I. Introduction

Diamond as a semiconductor in high-frequency, high-power transistors has unique advantages and disadvantages. Two advantages of diamond over other semiconductors used for these devices are its high thermal conductivity and high electric-field breakdown. The high thermal conductivity allows for higher power dissipation over similar devices made in Si or GaAs, and the higher electric field breakdown makes possible the production of substantially higher power, higher frequency devices than can be made with other commonly-used semiconductors.

In general, the use of bulk crystals severely limits the potential semiconductor applications of diamond. Among several problems typical for this approach are the difficulty of doping the bulk crystals, device integration problems, high cost and low area of such substrates. In principal, these problems can be alleviated via the availability of chemically vapor deposited (CVD) diamond films. Recent studies have shown that CVD diamond films have thermally activated conductivity with activation energies similar to crystalline diamonds with comparable doping levels. Acceptor doping via the gas phase is also possible during activated CVD growth by the addition of diborane to the primary gas stream.

The recently developed activated CVD methods have made feasible the growth of polycrystalline diamond thin films on many non-diamond substrates and the growth of single crystal thin films on diamond substrates. More specifically, single crystal epitaxial films have been grown on the {100} faces of natural and high pressure/high temperature synthetic crystals. Crystallographic perfection of these homoepitaxial films is comparable to that of natural diamond crystals. However, routes to the achievement of rapid nucleation on foreign substrates and heteroepitaxy on one or more of these substrates has proven more difficult to achieve. This area of study has been a principal focus of the research of this contract.

At present, the feasibility of diamond electronics has been demonstrated with several simple experimental devices, while the development of a true diamond-based semiconductor materials technology has several barriers which a host of investigators are struggling to surmount. It is in this latter regime of investigation that the research described in this report has and continues to address.

In this reporting period, (1) electron affinity and Schottky barrier height of thin Cu and Zr films on diamond (100) substrates were correlated by means of UV photoemission spectroscopy (UPS) measurements and (2) free standing, 4 mm diameter highly-textured (100) diamond membrane-based detectors were fabricated and used to measure the energy spectra of α-particles and to determine the spatial resolution of these particles. The following sections are self-contained in that they present an introduction, the experimental procedures, results and discussion, summary and indications of future research for the given research thrust.

II. Characterization of Metal-Diamond Interfaces: Electron Affinity and Schottky Barrier Height

A. Introduction

Negative electron affinity (NEA) surfaces based on wide band gap semiconductors such as diamond may be important for the development of cold cathode devices. However, n-type doping of diamond still poses a major challenge. The electron affinity of a semiconductor is defined as the energy difference between the vacuum level and the conduction band minimum. For most materials, the vacuum level lies above the conduction band minimum, corresponding to a positive electron affinity. Surfaces of wide band gap semiconductors such as diamond have the potential of exhibiting a NEA since the conduction band minimum lies near the vacuum level. For a NEA surface, the electrons from the conduction band minimum have sufficient energy to overcome the surface potential and can be emitted into vacuum.

Various surface treatments such as plasma cleaning, as well as annealing in ultra high vacuum (UHV), can shift the position of the vacuum level and, therefore, induce a NEA or remove it [1-6]. Pre-cleaning the diamond (100) samples with a wet chemical etch results in an oxygen termination of the surface. This chemisorbed oxygen layer forms a surface dipole that results in an increase in the surface workfunction. It is found that such a surface exhibits a positive electron affinity. Annealing these samples to 900°C–1050°C or exposing them to a H-plasma results in the removal of oxygen from the surface, a 2×1 reconstruction and a NEA [3, 5, 6]. The different threshold temperatures are related to different wet chemical pre-treatments [3]. It was found that 900°C was sufficient for samples pre-cleaned by an electrochemical etch. But 1050°C was required for a pre-clean employing chromic acid. The diamond (100) surface has been proposed to exhibit a monohydride termination subsequent to a 900°C–1050°C anneal or a H-plasma exposure. An H surface layer results in a dipole such that the work function is reduced, resulting in a NEA. Heating these samples to 1150°C resulted in a 2×1 reconstructed surface with a positive electron affinity [6]. This surface has been suggested to be free of adsorbates. In agreement with the experimental results, *ab initio* calculations for the 2×1 reconstructed surface predict a NEA for a monohydride terminated surface and a positive electron affinity for an adsorbate free surface [5].

Furthermore, it has been demonstrated that metals like Ti, Ni Co, Cu and Zr can induce a NEA on diamond surfaces [7-11]. In addition, no significant dependence of the Schottky barrier height on the metal work function has been found [3, 7-12]. Metal films deposited on adsorbate-free surfaces tend to result in lower Schottky barrier heights and lower electron affinities than for surfaces terminated by species such as hydrogen or oxygen [8, 9]. Photoemission spectroscopy is found to be a very sensitive method to determine whether a surface exhibits a NEA or not. Electrons get photoexcited from the valence band into states in

the conduction band and can quasi-thermalize to the conduction band minimum. Secondary electrons from the conduction band minimum appear as a sharp peak at the low kinetic energy end of photoemission spectra for NEA surfaces [13, 14].

Photoemission spectroscopy determines the emission properties of the surface itself. In comparison field emission data reflect a combination of carrier injection, transport and emission processes. In this study, diamond (100) surfaces have been cleaned by anneals to 1050°C or 500°C. Thin Cu or Zr films were deposited on these diamond substrates. The surface properties were characterized before and after metal deposition.

B. Experimental Details

The UHV system used in this study consists of several interconnected chambers including systems used for annealing, metal deposition, UPS and AES. Natural type IIb single crystal diamond (100) substrates (3.0 × 3.0 × 0.25 mm) were used. The samples were electro-chemically etched to remove non-diamond carbon and metal contaminants [15]. This etch included applying a DC bias of 350V between two Pt electrodes that were placed in deionized (DI) water as an electrolyte. The samples were suspended in water between the two electrodes. Following the electrochemical etch, a HF dip was employed to remove SiO_2 from the surface [3]. The wafers were then mounted on a Mo holder and transferred into the UHV system (base pressure ~1×10^{-10} Torr). As an *in vacuo* cleaning step, the wafers were annealed to 1150°C or 500°C for 10 minutes. This caused the pressure to rise to ~7×10^{-9} Torr. Subsequent to annealing, 2Å thick films of Cu or Zr were deposited by means of e-beam evaporation. The thickness of the metal layers was determined by a quartz crystal oscillator. During deposition, the pressure rose to ~2×10^{-9} Torr. Following the annealing and the growth steps, UPS and AES were employed to analyze the surface properties.

The presence of a Cu or Zr film was confirmed by using AES. AFM images of the diamond wafers clearly showed arrays of linear groves parallel to each other with a depth of ~20 Å. This surface structure is due to the commercial polishing of the samples. No island structures were observed in AFM measurements after 2 Å of deposition, which may be indicative of a uniform 2D layer for both Cu and Zr.

HeI (21.21 eV) radiation was used to excite the photoemission of electrons. A 50 mm hemispherical analyzer was employed to measure the emitted electrons with an energy resolution of 0.15 eV. A bias of 1V was applied to the sample to overcome the workfunction of the analyzer and, thus, to detect the low energy electrons emitted from the NEA surface. The position of the sharp NEA peak at the low energy end of photoemission spectra corresponds to the energy position of the conduction band minimum, E_C. Emission from E_C is positioned at $E_V + E_G$ in the spectrum, where E_V is the energy of the valence band maximum and E_G that of the bandgap. Emission from the valence band maximum appears at $E_V + h\nu$ in the

spectrum. The spectral width or the distance between emission from the valence band maximum and the conduction band minimum is therefore $h\nu - E_G$. With the values for He I radiation $h\nu = 21.21$ eV and the bandgap of diamond $E_G = 5.47$ eV a spectral width of ~15.7 eV is determined for a NEA surface. However, for the case of a positive electron affinity surface, the low energy cutoff will be determined by the position of the vacuum level and the spectral width will be smaller.

The base pressure in the field emission chamber was $\sim 2\times10^{-7}$ Torr. To determine the current–voltage characteristics, a bias of 0 to 1100V was applied between the sample and a 2 mm diameter platinum anode with a rounded tip. The distances were varied between 2 and 20 μm.

C. Results and Discussion

AES spectra of the as-loaded samples exhibited features indicative of the presence of oxygen on the surface. Following a 500°C anneal, the oxygen feature was only slightly reduced. Upon heating the samples to 1150°C, oxygen could no longer be detected by means of AES. By employing UPS, positive electron affinities of $\chi \cong 1.4$ eV and of $\chi \cong 0.7$ eV were observed for the crystals annealed to 500°C and 1150°C, respectively. These values correspond to previous results [5, 9]. Oxygen chemisorbed to diamond is expected to induce a stronger surface dipole and, therefore, cause an increase in the workfunction compared to a clean surface. Our results are consistent with this idea. Upon deposition of 2Å of copper on clean surfaces, a Schottky barrier height of $\Phi_B \cong 0.70$ eV and a NEA were observed by UPS (Fig. 1a). In comparison, depositing 2Å of Cu onto oxygen terminated diamond (100) surfaces resulted in a positive electron affinity of $\chi \cong 0.75$ eV, and a corresponding Schottky barrier of $\Phi_B \cong 1.60$ eV was obtained (Fig. 1b). Depositing 2Å of Zr onto clean diamond (100) samples resulted in a Schottky barrier height of $\Phi_B \cong 0.7$ eV and a NEA (Fig. 2a). Emission below the conduction band minimum E_C was observed. Subsequent to deposition of 2Å of Zr on oxygen terminated diamond (100) surfaces, a NEA was observed. A larger Schottky barrier height of $\Phi_B \cong 0.9$ eV was measured (Fig. 2b). These results are summarized in Table I. Equation 1 gives an expression for the electron affinity of a p-type semiconductor subsequent to metal deposition [16],

$$\chi = (\Phi_M + \Phi_B) - E_G. \qquad (1)$$

Using the workfunction of Cu for the (100) surface $\Phi_M = 4.59$ eV, the bandgap of diamond $E_G = 5.47$ eV and the measured Schottky barrier heights one can calculate the electron affinities of $\chi \cong -0.18$ eV for the clean surface and $\chi \cong 0.72$ eV for the oxygen terminated surface. With the value of $\Phi_M = 4.05$ eV for the workfunction of Zr and the

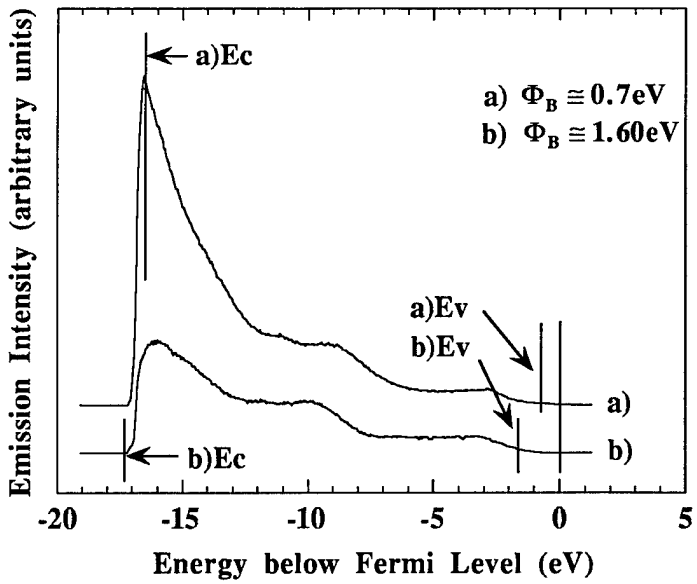

Figure 1. UV photoemission spectra of 2Å of Cu grown on a diamond (100) surface following an anneal to a) 1150°C b) 500°C. A metal induced NEA is observed for a) whereas a positive electron affinity is detected for b).

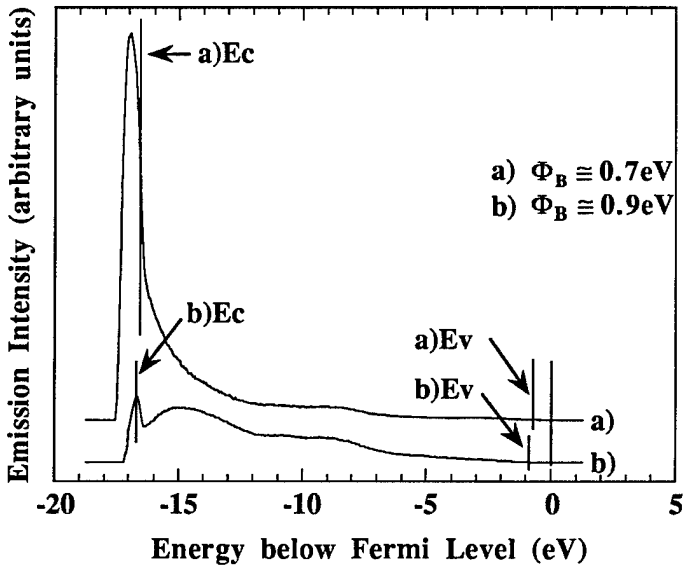

Figure 2. UV photoemission spectra of 2Å of Zr deposited on a diamond (100) surface annealed to a) 1150°C b) 500°C. Metal induced NEA's are observed upon deposition of Zr for both a) and b). For a) emission below E_C is detected.

Table I. Results of Electron Emission Measurements

Sample	UPS	Field Emission Threshold (V/μm)	Barrier Height (eV)
C(100)	after 500°C anneal PEA, $\chi \cong 1.4$ eV	79 ± 7	0.23 ± 0.01
Cu/C(100) clean	NEA, $\chi < 0$, $\Phi_B \cong 0.70$ eV	25 ± 3	0.10 ± 0.01
Cu/C(100) oxygen	PEA, $\chi \cong$ 0.75 eV, $\Phi_B \cong 1.60$ eV	53 ± 4	0.21 ± 0.01
Zr/C(100) clean	NEA, $\chi < 0$, $\Phi_B \cong 0.7$ eV	20 ± 3	0.09 ± 0.01
Zr/C(100) oxygen	NEA, $\chi < 0$, $\Phi_B \cong 0.9$ eV	49 ± 4	0.20 ± 0.01

PEA: positive electron affinity, NEA: negative electron affinity. The averages and standard deviations of the field emission measurements at different distances are shown as the field emission threshold and the barrier height. The threshold current is 0.1 μA.

observed Schottky barrier heights electron affinities of $\chi \cong$ - 0.72 eV for the clean surface and $\chi \cong$ - 0.52 eV for the oxygen terminated surface are obtained. These results are in agreement with the NEA and positive electron affinity effects that were observed by means of UPS. The emission detected below E_c for Zr on the clean surface is consistent with the calculated value of $\chi \cong$ - 0.72 eV. The fact that no emission below E_c was observed for Zr on oxygen terminated diamond may be due to a different interface structure. It has been reported that carbon contaminants lower the workfunction of Ni [17]. The workfunction of the 2Å thick films in our study may be affected by the carbon of the diamond. But such an effect would only lead to a stronger NEA effect for Cu on the clean surface and both Zr on the clean and oxygenated surface and would be consistent with our results. For Cu on the oxygen-terminated surface, the measured and calculated values for the electron affinity are consistent with each other. Thus, at least for the latter case, this effect is not expected to be significant.

For systems like Ti or Ni layers on diamond (111) surfaces [7, 8] this simple workfunction model has been used successfully to explain NEA or positive electron affinity effects. It has been observed that Ni deposited on an adsorbate free (111) surface induced a NEA [8]. In comparison, a positive electron affinity and a larger Schottky barrier were obtained for thin Ni films on (111) surfaces terminated by hydrogen. In theoretical studies by Erwin and Pickett [18-21] and Pickett, Pederson and Erwin [22], it was reported that the most stable

configuration for Ni on clean (111) and (100) surfaces resulted in a Schottky barrier height of less than 0.1 eV. Regarding copper on diamond (111) surfaces, Lambrecht [23] obtained a value for the Schottky barrier height of less than 0.1 eV for clean surfaces and greater than 1.0 eV for hydrogen-terminated surfaces. According to these results, the interface termination appears to be crucial for the Schottky barrier height. For metals deposited on clean surfaces, lower values for the Schottky barrier height and a greater likelihood of inducing a NEA are expected than for metals on non adsorbate free surfaces. The Schottky barrier heights reported in this study for Cu and Zr on diamond are in agreement with this. Zr and Ti have a stronger affinity to C than is the case for Cu and Ni. This may play a role in the interface formation of the thin films on diamond. Both Zr or Ti on clean as well as oxygen-terminated diamond surfaces tend to exhibit lower electron affinities than Cu or Ni on corresponding surfaces. This can be determined from the results of this study, as well as previous reports [7, 8]. The workfunction of Ti is only 0.3 eV higher than that of Zr. Apparently the relatively small difference between Zr and Ti is sufficient to induce a NEA for Zr on the oxygen terminated surface but not for the case of Ti. It is significant that a metal induced NEA was observed for deposition of Zr on both clean and oxygen terminated surfaces. Prior to this work only low workfunction metals like Cs have been found to induce a NEA on non adsorbate fee diamond surfaces [24].

Field emission measurements were performed on diamond samples and on Cu or Zr films deposited on clean and oxygen terminated diamond surfaces. For a current of 0.1 μA, values between 20 and 79 V/μm were measured for the emission threshold field. A summary of the results is shown in Table I. Previous studies have reported comparable values for diamond samples [11, 25, 26]. As an example, I-V curves for the diamond surface are shown in Fig. 3. For comparison, one I-V curve for Zr on a clean diamond surface has been included also. These results have been compared to the Fowler–Nordheim equation [27]:

$$I = k\left(\frac{V}{d}\right)^2 \exp\left(\frac{-6530 d\varphi^{3/2}}{V}\right). \qquad (2)$$

I is the current in amps, V is the bias in volts, d is the distance between the sample and the anode in microns, k is a constant and φ is the effective barrier height in eV. The field enhancement factor has been neglected since the surfaces have been found to be essentially flat by means of AFM. The effective barrier heights φ were obtained by fitting the field emission data to Eq. 2 (see Table I). Depositing Cu or Zr onto both clean and oxygen-terminated diamond (100) surfaces improves the emission properties. The case of Zr on clean surfaces gave the best results. Both UPS and field emission measurements show these trends consistently.

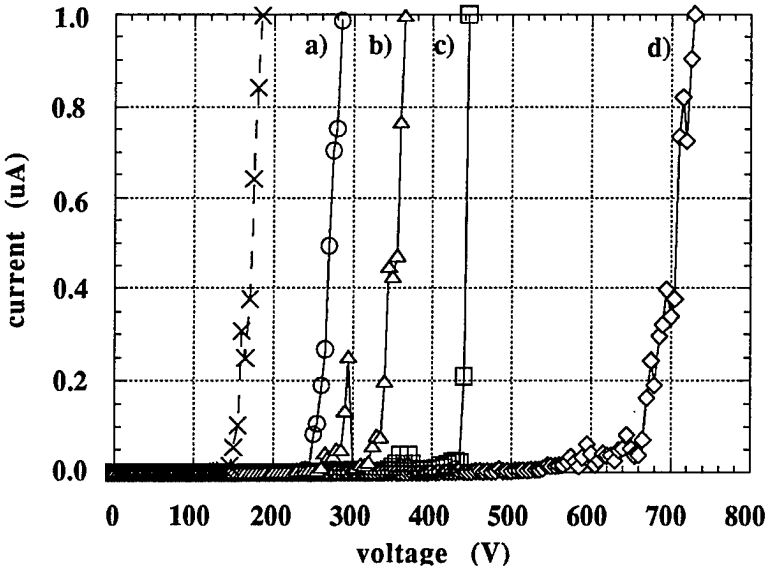

Figure 3. Field emission current–voltage curves for a type IIb single crystal diamond (100) sample. Distances between the sample and the anode: a) 3.3 μm, b) 4.3 μm, c) 5.6 μm, d) 8.5 μm. For comparison one current–voltage curve for Zr on a clean diamond (100) surface is also shown (dashed line) with a distance between the sample and the anode of 7.8 μm.

D. Conclusions

The effects of depositing thin metal films onto clean and oxygen terminated diamond (100) substrates has been studied by UPS. Cu only induced a NEA on clean surfaces. In comparison, Zr induced a NEA on both clean and oxygen terminated surfaces. Emission even below E_c was detected for Zr on clean surfaces. Both the field emission threshold and the effective barrier height were reduced in a manner consistent with the UPS results by depositing metals on diamond.

E. Future Work

Work in the future will involve the fabrication and characterization of electron injecting contacts. In addition, investigation of the electron emission mechanism is planned.

F. References

1. F. J. Himpsel, D. E. Eastman, P. Heimann and J. F. van der Veen, Phys Rev. B **24**, 7270 (1981).
2. B. B. Pate, M. H. Hecht, C. Binns, I. Lindau and W. E. Spicer, J. Vac. Sci. Technol. **21**, 364 (1982).
3. P. K. Baumann, T. P. Humphreys and R. J. Nemanich, in *Diamond, SiC and Nitride Wide Bandgap Semiconductors*, edited by C. H. Carter, G. Gildenblat, S. Nakamura, R. J. Nemanich, (Mater. Res. Soc. Proc. **339**, Pittsburgh, PA, 1994) 69-74.
4. J. van der Weide and R. J. Nemanich, Appl. Phys. Lett. **62**, 1878 (1993).
5. J. van der Weide, Z. Zhang, P. K. Baumann, M. G. Wensell, J. Bernholc and R. J. Nemanich, Phys. Rev. B **50**, 5803 (1994).

6. P. K. Baumann and R. J. Nemanich, *Proc. of the 5th European Conference on Diamond, Diamond-like and Related Materials*, edited by P. K. Bachmann, I. M. Buckley-Golder, J. T. Glass, M. Kamo: J. Diamond Rel. Mat., **4** (1995) 802.
7. J. van der Weide and R. J. Nemanich, J. Vac. Sci. Technol. B **10**, 1940 (1992).
8. J. van der Weide and R. J. Nemanich, Phys. Rev. B, **49**, 13629 (1994).
9. P. K. Baumann and R. J. Nemanich, Appl. Surf. Sci., in press.
10. P. K. Baumann and R. J. Nemanich, in *Diamond for Electronic Applications*, edited by C. Beetz, A. Collins, K. Das, D. Dreifus, T. Humphreys, P. Pehrsson, (Mater. Res. Symp. Soc. Proc. **416**, Pittsburgh, PA 1996) 157-162.
11. P. K. Baumann, S. P. Bozeman, B. L. Ward and R. J. Nemanich in III-Nitride, *SiC, and Diamond Materials for Electronic Devices*, edited by C. Brandt, D. K. Gaskill, R. J. Nemanich, (Mater. Res. Soc. Proc., Pittsburgh, PA , 1996), in press.
12. P. K. Baumann, T. P. Humphreys, R. J. Nemanich, K. Ishibashi, N. R. Parikh, L. M. Porter and R. F. Davis, Proc. of the 4th European Conference on Diamond, Diamond-like and Related Materials, edited by P. K. Bachmann, I. M. Buckley-Golder, J. T. Glass, M. Kamo: J. Diamond Rel. Mat. **3** (1994) 883.
13. F. J. Himpsel, P. Heimann and D. E. Eastman, Sol. State Commun. **36**, 631 (1980).
14. B. B. Pate, W. E. Spicer, T. Ohta and I. Lindau, J. Vac. Sci. Technol. **17**, 1087 (1980).
15. M. Marchywka, P.E. Pehrsson, S.C. Binari and D. Moses, J. Electrochem. Soc., **140**, (2), L19 (1993).
16. E. H. Rhoderick and R. H. Williams, *Metal-Semiconductor Contacts* Clarendon, Oxford, (1988).
17. C. Weiser, Surf. Sci. **20**, 143 (1970).
18. S. C. Erwin and W. E. Pickett, Surf. Coat. Technol. **47**, 487 (1991).
19. S. C. Erwin and W. E. Pickett, Solid State Commun. **81**, 891 (1992).
20. W. E. Pickett and S. C. Erwin, Phys. Rev. B **41**, 9756 (1990).
21. W. E. Pickett and S. C. Erwin, Superlatt. Microsruct. **7**, 335 (1990).
22. W. E. Pickett, M. R. Pederson and S. C. Erwin, Mater. Sci. Eng. B **14**, 87 (1992).
23. W. R. L. Lambrecht, Physica B **185**, 512 (1993).
24. M. W. Geis, J. C. Twichell, J. Macaulay, K. Okano, Appl. Phys. Lett. **67**, 1 (1995).
25. W. Zhu, G. P Kockanski, S. Jin and L. Siebels, J. Appl. Phys., in press.
26. S. P. Bozeman, P. K. Baumann, B. L. Ward, M. J. Powers, J. J Cuomo, R. J. Nemanich and D. L Dreifus, *Proc. of the 6th European Conference on Diamond, Diamond-like and Related Materials*, edited by P. K. Bachmann, I. M. Buckley-Golder, J. T. Glass, M. Kamo: J. Diamond Rel. Mat. (1996), 802.
27. R. Gomer, *Field Emission and Field Ionization*, Cambridge, MA, (1961).

III. Fabrication and Testing of a Diamond Microstrip Particle Detector

A. Introduction

Since conventional silicon detectors can easily be destroyed in high-energy and high-radiation environments such as α and e^- beam, new materials are desired. Diamond is an enticing candidate for high-energy particle detection due to its superior properties [1, 2]. For example, diamond has thermal conductivity six times greater than Cu and has high radiation hardness. Thus, a diamond detector can be exposed directly to a high-intensity beam without suffering significant thermal or radiation damage. Diamond also has high breakdown voltage and electrical resistivity. Due to these properties, high electric fields can be applied to diamond without significant increase in leakage current and simple metal-diamond-metal structure can be used (see Fig. 1) instead of reverse pn junction structure for conventional silicon detector. Table I summarizes the relevant properties of diamond and compares with the silicon.

Because grain boundaries are transport barriers and can degrade device performance, single crystal diamond films are needed. Although economically viable size and quantities of single-crystal diamond films are not available, there has been significant progress on highly textured diamond films [3-5]. Since the detector signal is collected vertically, single crystallinity can be mimicked in collection direction by producing a textured film. In order to improve the collection distance and electrode contact, highly-oriented (100)-texture diamond films are desired. By coupling the bias enhanced nucleation (BEN) and van der Drift "evolutionary selection" process [6], one can produce highly-textured (100) diamond films.

Texture growth can be understood as a growth competition between differently oriented crystals. Thus, the primary factor that controls film texture is the growth velocity in the substrate normal direction. According to the van der Drift "evolutionary selection" growth process [6], the crystals with the direction of fastest growth perpendicular to the substrate will have fastest vertical growth rate. Those crystals will overgrow other crystals and eventually survive at the surface. The growth of a polycrystalline CVD diamond starts from differently oriented nuclei. Since (100)-texture oriented nuclei have their fastest growth direction perpendicular to the silicon (100) substrate, these (100)-texture nuclei will over grow and survive at the surface as the films grows, as shown in Fig. 2. To achieve a fully textured film with minimal thickness, an initial layer width a high density of similarly textured crystals is necessary. A bias enhanced nucleation procedure has been developed for the MPCVD system [7] that can produce a nucleation density of about $10^{10}cm^{-1}$ and a high density of nuclei that have crystal directions closely oriented to the substrate. These highly textured grains will quickly overgrow neighboring "misaligned" grains and grain boundary elimination is possible as adjacent oriented crystals coalesce.

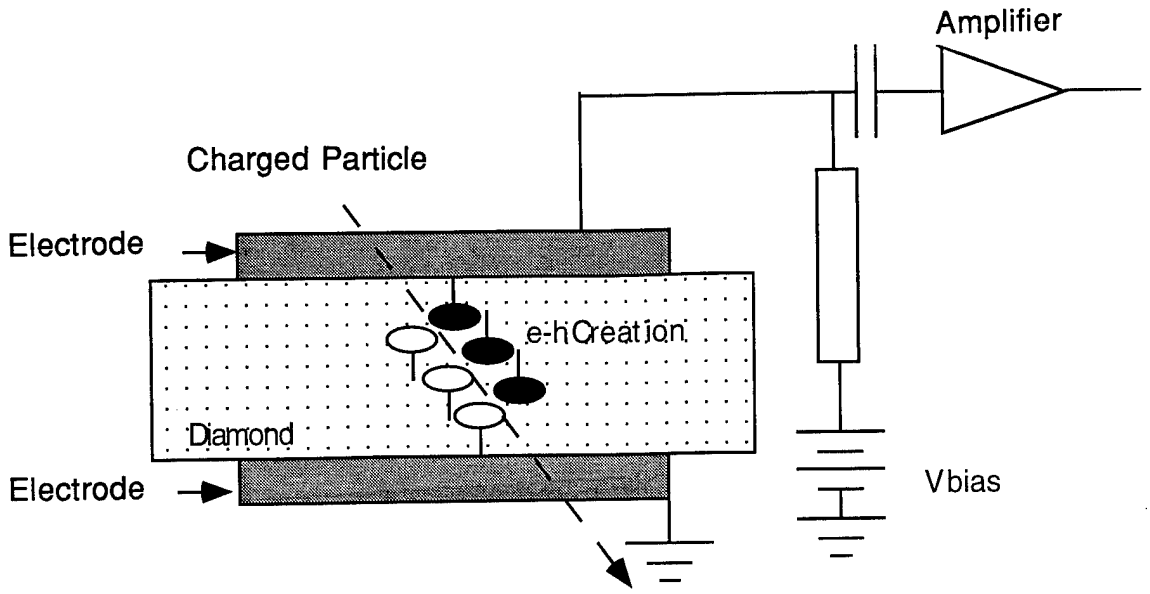

Figure 1. Schematic view of the diamond detector.

Table I. Selected Properties of Diamond for Use in High Energy Particle Detector. Properties of Si are Included for Comparison [1,2].

Property	Diamond	Silicon
Thermal conductivity	2000 W/m-K	139 W/m-K
Band gap	5.5 eV	1.1 eV
Electrical resistivity	$>10^{11}$ Ω-cm	10^5 Ω-cm
Breakdown voltage	10^7 V/cm	10^3 V/cm
Electron mobility	1800 cm^2/V-s	1500 cm^2/V-s
Hole mobility	1500 cm^2/V-s	500 cm^2/V-s
Carrier saturation velocity	220 μm/ns	100 μm/ns

Once the initial diamond layer has been formed, maintaining the correct crystal growth direction is crucial. Previous experiments in a LPCF reactor have demonstrated that control of the diamond crystal growth direction can be easily maintained [8]. Highly textured (100) diamond films have been fabricated by a joint MPCVD and LPCF technique [9]. The LPCF system reduces processing time due to its high growth rate, 4~5 μm/hr.

B. Experimental Procedure

Diamond Deposition. Single crystal silicon (100) was used as a substrate. The substrate was cleaned by acetone, methanol, and isopropanol. After the cleaning, the substrate was etched in dilute HF acid to remove any oxide on substrate surface. In the MPCVD system, the substrate went through a four-step deposition process. This process consisted of a hydrogen

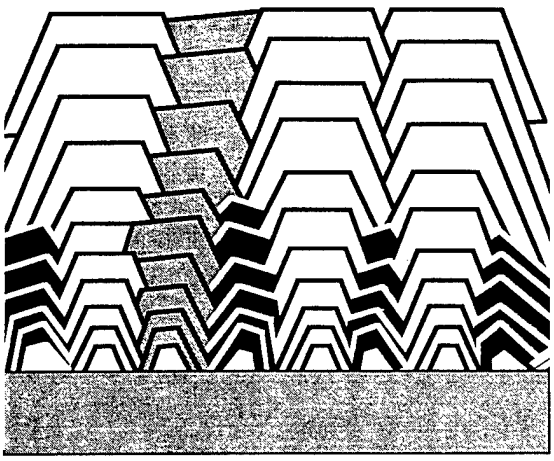

Figure 2. Schematic representation of "evolutionary selection" texture growth process.

plasma clean, surface carburization, BEN, and growth, see Table II. Hydrogen plasma cleaning was performed to remove any carbonaceous residue on the substrate. Following the hydrogen plasma clean, the carburization step was undertaken to carburize the silicon substrate at high temperature and methane/hydrogen plasma. After the carburization step, diamond was nucleated via the BEN process. During the BEN, a negative DC voltage was applied to the substrate in order to increase the carbon flux and reaction at the substrate surface. At the end of the step, the bias voltage was terminated and the system parameters were changed to the appropriate oriented growth condition. The growth step was performed so that the initial diamond layer could be observed in the SEM to confirm the growth texture. The sample was then transferred to the LPCF reactor for the final growth step. Under the LPCF system, C_2H_2/O_2 flame was used to deposit a 15μm diamond film at reduced pressure (~47 Torr). The deposition temperature was 760°C as measured by a two-color infrared pyrometer (Williamson, Inc.).

Device Fabrication. The front electrodes, Ti and Au, were fashioned in a microstrip pattern with thickness of 500Å and 2000Å, respectively. An initial layer of Ti was used to improve adhesion and ohmic contact with the diamond film [10,11]. After the deposition of front electrodes, silicon was removed to form a free-standing, 4 mm diameter, diamond membrane. Most of silicon was mechanically removed by dimpling, and the remaining silicon was preferentially etched in a KOH solution. During the chemical etching step, front electrodes were protected by a chemically resistant wax. The same electrode metal and thickness was used for the back electrode. After the back electrode deposition, the sample was annealed at 500°C for 30 min. to improve the contact between the Ti and diamond.

Device Testing. The fabricated detector was transferred to CEBAF and was tested to measure the energy spectra of α particle from a ^{241}Am source and the beam current was

200mA which was produced to a characteristic α particles energy of 5.5MeV. The detector was perpendicular to a horizontal α particle beam with a 1 cm gap between the α-source and detector, as shown in Fig. 3.

C. Results and Discussion

The (100) textured diamond film was produced as outlined in experimental procedure. Figure 4(a,b) shows the surface morphologies of MPCVD and LPCF grown diamond films, respectively. Scanning electron microscopy examination of the initial diamond film after deposition in the MPCVD system showed a nucleation density of 10^{10}/cm. A cursory examination of the micrographs revealed that approximately 40% of the diamond grains were oriented to each other. After deposition in the LPCF reactor, all of the "misaligned" grains were overgrown and a fully textured film was produced. A few diamond grains appeared to have coalesce and formed low-angle grain boundaries.

Table II. Summary of System Parameters

Parameters	H_2 Plasma Clean	Carburization	BEN	Growth in MPCVD	Growth in LPCF
Power	600 W	750 W	600 W	750 W	
Pressure	25 Torr	30 Torr	20 Torr	30 Torr	47 Torr
Gas ratio	-	CH_4/H_2=0.2	CH_4/H_2=0.52	CH_4/H_2=0.002	C_2H_2/O_2=1.0
Bias Current	-	-	50 mA	-	
Bias Voltage	-	-	-210 V	-	
Temperature	700°C	900°C	900°C	800°C	760°C
Duration	30 min.	60 min.	60 min.	13 hr.	3 hr.

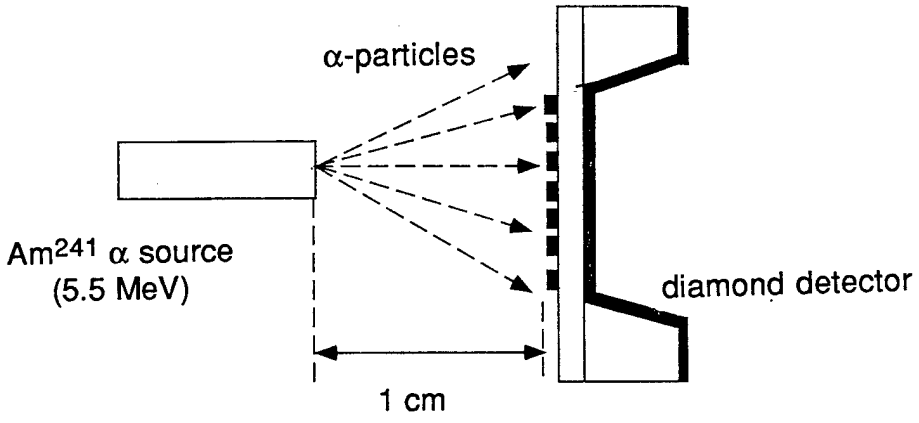

Figure 3. Schematic illustration of diamond particle detector and its position to the incoming beam. The α-particle source was ^{241}Am with a characteristic energy of 5.5MeV

(a)

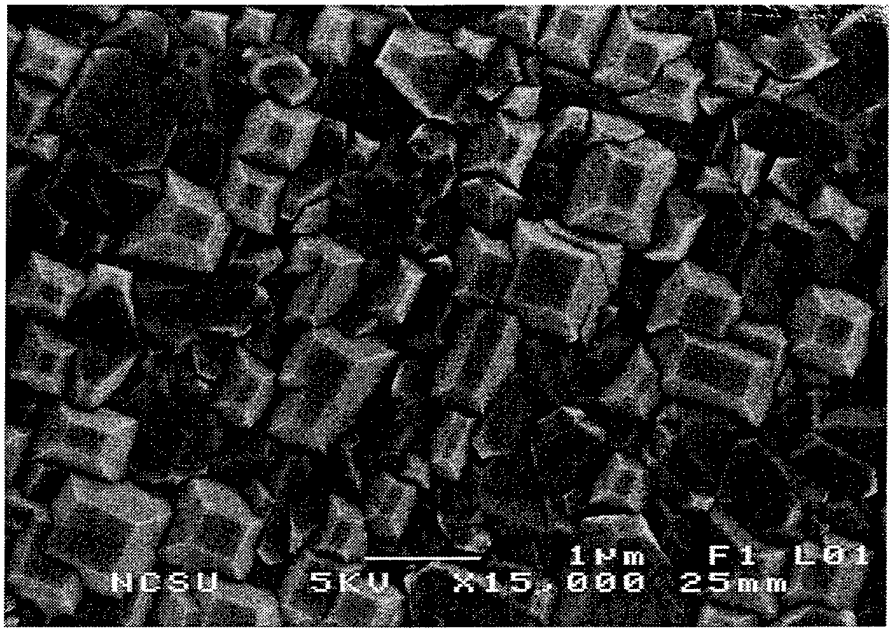

(b)

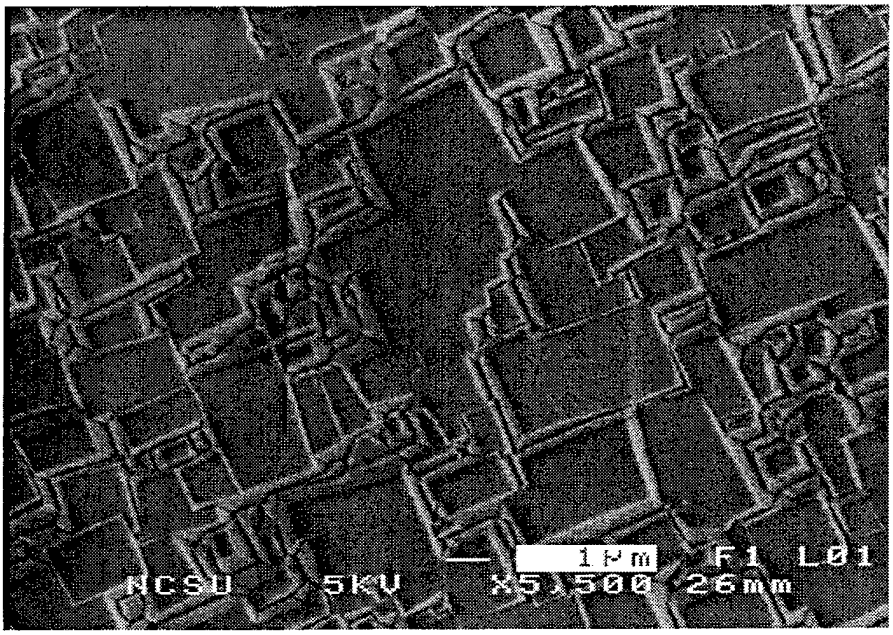

Figure 4. (a) Morphology of MPCVD grown diamond film and (b) morphology of MPCVD nucleated LPCF grown diamond film.

Testing the Detector. The detector measured energy spectra of α-particles at CEBAF in two different environments: vacuum and air (see Fig. 5). Since the incoming beam radius of α-particles (5 mm) was much larger than width of electrode (100 μm), small fraction of particles vertically penetrated into the electrode while most α-particles went through the detector with various angles (Fig. 2). Only those particles that penetrated the electrode vertically were responsible for the characteristic energy of α-particles, 5.5 MeV, and a small fraction of energy was absorbed by those particles with various incident angles. Therefore, the intensity at 5.5 MeV was small and the peak was shifted to lower energies for both experiments. Due to the scattering of α-particles in air, the detector showed significant reduction in peak intensity and broad secondary peak at low energy.

D. Conclusions

The diamond microstrip particle detector has been fabricated and measured the energy spectrum of 5.5 MeV α particles. In order to utilize the superior qualities of diamond, such as high thermal conductivity, radiation hardness and electrical resistivity, highly textured (100) diamond film was used as the detector material. The textured diamond film was obtained by coupling BEN, in a MPCVD system, and an "evolutionary selection" growth process, in a LPCF system. Following the textured diamond film deposition, the silicon substrate was etched to form a free-standing diamond membrane. Microstrip electrodes were patterned to measure the energy spectra and position the incoming particles. The fabricated detector analyzed α particles at CEBAF and the device performance was comparable to single crystalline detectors.

E. Future Research Plans and Goals

In order to obtain a higher quality of textured diamond film, further optimization for (100) texture deposition conditions is needed for the MPCVD and LPCF systems. Additional experiments will use an e-beam to measure the energy spectra and position of the incoming particles.

F. References

1. M. Franklin, *et al.*, Nuclear Instruments and Methods A **315**, 39 (1992).
2. H. Kangan, *et al.*, 2nd International Conference on the Applications of Diamond Films and Related Materials, 29 (1993).
3. C. Wild, *et al.*, Diamond and Related Materials **2**, 158 (1993).
4. C. Wild, *et al.*, Diamond and Related Materials **3**, 373 (1994).
5. B.A Fox, *et al.*, Diamond and Related Materials **3**, 382 (1994).
6. A. Van der Drift., Philips Research Report **22**, 267 (1967).
7. S. D. Wolter, *et al.*, Applied Physics Letters **62**, 1215 (1993)
8. C. A. Wolden, *et al.*, Applied Physics Letters **69**, 2258 (1996).
9. C. A. Wolden, *et al.*, Materials Letters (submitted, Nov. 1996).
10. T. Tachibana, *et al.*, Physical Review B 45 **11**, 975 (1992).
11. H. Shiomi, *et al.*, Japanese Journal of Applied Physics **28**, 758 (1989).

(a)

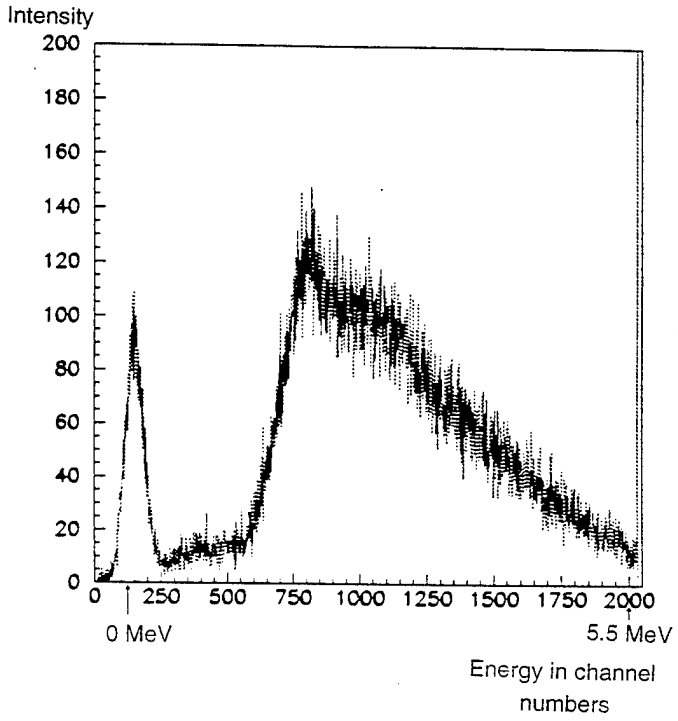

(b)

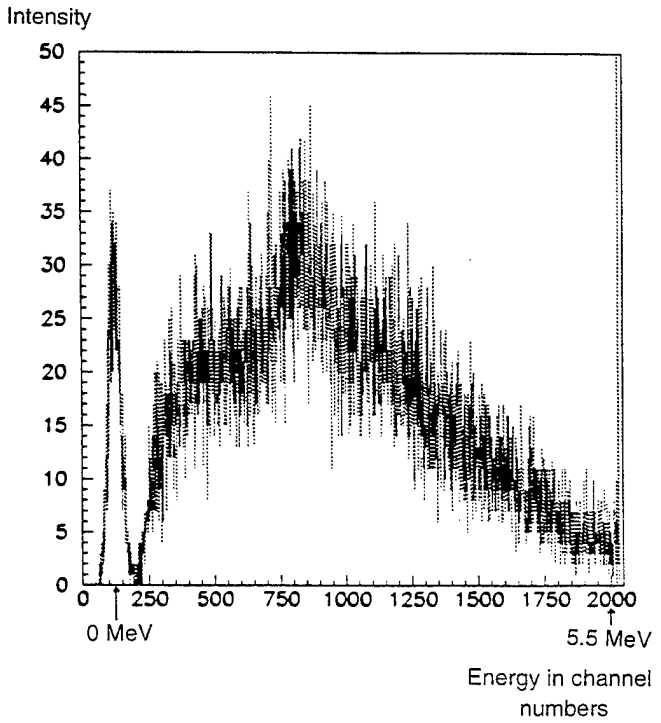

Figure 5. a) Energy spectrum of 5.5 MeV α particles in vacuum and b) energy spectrum of 5.5 MeV α particles in air.

IV. Distribution List

Dr. Colin Wood Office of Naval Research Electronics Division, Code: 312 Ballston Tower One 800 N. Quincy Street Arlington, VA 22217-5660	3
Administrative Contracting Officer Office of Naval Research Regional Office Atlanta 101 Marietta Tower, Suite 2805 101 Marietta Street Atlanta, GA 30323-0008	1
Director, Naval Research Laboratory ATTN: Code 2627 Washington, DC 20375	1
Defense Technical Information Center 8725 John J. Kingman Road, Suite 0944 Ft. Belvoir, VA 22060-6218	2